IJCRT.ORG ISSN : 2320-2882

INTERNATIONAL JOURNAL OF CREATIVE RESEARCH THOUGHTS (IJCRT)

An International Open Access, Peer-reviewed, Refereed Journal

Numerical Simulation Of Piezoelectric Sensor Performance For Structural Health Monitoring Applications

Rahul Kumar[1], Bal Kishan Yadav[1], Anuj Verma[2]

[(1)]M.Tech scholar, Rajshree Institute of management and Technology, Bareilly

[(2)]Professor,(HOD) Department of Civil Engineering, Rajshree institute of management and Technology, Bareilly

Abstract:- Since collapse might harm public safety and the economy, building and construction structures must be maintained. Critical structures need periodic inspections to fix issues. Visual examination is tough and knowledge-intensive yet recommended. Better, more reliable monitoring is needed. The study uses high-frequency monitoring to discover structural problems low-frequency methods overlook. PZT patches detect and create signals. These patches can detect small structural behaviour changes that indicate problems. Check structural data against prior data to find research gaps. In this study, high-frequency EMI methods identify minute structural differences. We tested our methods in a scaled reinforced concrete lab. Computer models described observable phenomena for experimentation. Computational models anticipate damage and fracture propagation. Compared to empirical testing, predictive testing saves time and money. Computational modelling can assess structural typologies' environmental and fracture propagation mechanical responses. This study implies computational tools improve structural monitoring and construction engineering.

Keywords: Structural health monitoring, Smart structures, Sensor technology, Numerical Simulation, Automated inspection.

1. Introduction

Smart structures with sensing, actuation, and control may change structural engineering. These structures sustain people, loads, and surrounds. Smart materials use has increased due to structural changes. Vibration dampening, energy harvesting, form control, and structural health monitoring are civil engineering study areas. See references [1–3]. Advanced materials make infrastructure design, construction, and maintenance greener. Assess structural health using loads and crucial reactions. Testing performance, operational issues, degradation, and structural integrity before and after heavy operations is standard. Reference [4]. Recently, civil engineers emphasised health monitoring. Applying it to civil infrastructure is hard. Applying theory requires controlled experimentation. These are needed for civil infrastructure monitoring. Investigation ongoing. These issues and cross-disciplinary collaboration can enhance infrastructure durability and sustainability through structural health monitoring.

Quality health monitoring is multifaceted. Set technology health and performance indicators first. Farra et al. studied health and performance evaluation system damage prognosis [5]. This data helps engineers and academics monitor infrastructure health. Data, sensors, and wireless connectivity enable health monitoring [6]. These technologies must fulfil structural health and performance criteria during development, testing, and deployment. Yao says that environment, human error, and external factors destroy structures [7]. Better to see industrial, bridge, and building decay. A costly, time-consuming, and individual process. Modern sensors and

data collectors detect flaws faster and enable preventative maintenance. Technology may increase structural health monitoring accuracy, reliability, and cost-effectiveness, protecting infrastructure investments. Global population growth requires public infrastructure. Civil engineering infrastructure must be repaired for safety due to age and natural disasters. SHM graduated from aerospace and mechanical in the late 1970s to civil. SHM assesses structural health faster and cheaper than maintenance [8].

SHM passively and actively monitors civil infrastructure. Unactuated passive monitoring detects structural responses to external stimuli. Acoustic emissions and vibration differences indicate degradation; therefore, it works. Modal analysis and ambient vibration testing show structural growth [9-11].For focused system dynamics inquiry, active monitoring creates regulated excitation pulses and structural reactions. Modal, impact, and acoustic emission tests measure damage reactions [12]. These methods detect minor structural changes to detect damage [13].

Self-healing and self-repairing mechanisms are revolutionising structural engineering by making infrastructure more resilient. These novel methods diagnose and fix construction issues without humans. Microcapsules or vascular networks with healing agents improve mechanical properties and structural lifetime [14-19]. Smart materials and sensors improve the environment [20-21]. These approaches reduce upkeep and make constructions waterproof and disaster-resistant [22]. General building improvements need additional research.

SHM analyses civil infrastructure dynamics through dynamic response. Structure, performance, and health are affected by seismic, wind, and traffic vibrations [23]. We employ natural frequencies, mode shapes, damping ratios, and dynamic displacements. Modal analysis demonstrates a structure's inherent frequencies, mode shapes, stiffness, mass distribution, and damping under dynamic stresses [24]. In normal operation, ambient vibration data monitors structural behaviour and condition without stimulation [25]. In dynamic response data, wavelet, frequency domain, and time-frequency analysis can reveal structural degeneration [26-27]. Dynamic response-based building maintenance, repair, and retrofitting improve safety, dependability, resilience, and sustainability [28].

SHM with static responses shows civil infrastructure behaviour. Measurements of displacements, strains, and stresses reveal structural degradation under changing loads [29]. Engineers use strain gauges or extensometers to detect damage-causing deformation or stress [30-31]. Sensor deflections show stiffness and structure. Finite element analysis (FEA) predicts structural reactivity to loads for proactive health evaluation [32]. Compared simulated and measured outcomes verify models and reveal maintenance needs [33]. These methods guide maintenance, repair, and retrofitting decisions to ensure structural safety, dependability, durability, and built environment resilience and sustainability.

This project aimed to develop finite element analysis (FEA) methods for intelligent structures, focusing on comparing experimental health monitoring results of a laboratory-scale Reinforced Concrete (RC) frame with FEA simulations. High-frequency dynamic response using piezoceramic (PZT) actuators and sensors detected early damage signs. Numerical simulations closely matched experimental data, determining damping constants and analysing damage effects efficiently. This approach streamlines future research by reducing time and resource costs while effectively examining structural health and integrity of smart buildings through numerical modelling.

This work uses numerical methods to analyse a small-scale reinforced concrete (RC) frame. Our study is based on Bhalla and Soh's 2004 experimental investigation [34]. We started our endeavour by acquiring an initial conductance signature for the numerical RC frame to prepare for our investigations. Our numerical model was enhanced, and damage simulations were added in the second phase. This lets us study how different types of damage impact the RC frame's structural integrity and reaction. We use numerical simulations and experimental data to better understand RC structures' behaviour under diverse situations. Table 1 provides basic concrete properties for study. Table 2 shows PZT patch parameters that are important for understanding its behaviour in the investigation.

Table1. Material properties of concrete

Parameter	Value
Young's Modulus	2.74×10^4 MPa
Density	2400 kg/m^3
Stiffness Damping Factor	1.5×10^{-8}
Mass Damping Factor	0.001
Poison's Ratio	0.3

Table 2. Electrical and mechanical properties of PZT

Parameter	Value
Density	7800 kg/m3
Young's Modulus, Y_{11}^E	6.667 × 1010 MPa
Mechanical loss factor, η	0.001
Dielectric constant, ε_{33}^T	332.124 ×10-8
Piezoelectric constant, d31	-2.1 × 10-10 mV-1
Dielectric loss factor, δ	0.015

2. Modelling of Smart Structures

Experimental reinforced concrete (RC) frame in Figure 1. This picture illustrates the researched structure. The frame model was created in Ansys 9. The model comprises 42, 10-mm solid planar parts. PZT patch 2 received two 100-kN harmonic forces to replicate the frame's piezoceramic load. For clarity, the PZT patch was beam centre. To match experimental frame, boundary conditions were reproduced. The experimental frame's left side is modelled in 2D finite elements in Figure 2. Visualising the simulation and structural setup may assist.

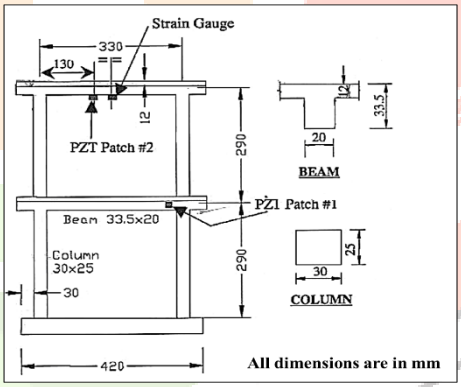

Figure 1. The test frame [34].

$$z = \frac{\bar{F}}{i\omega \bar{X}} \tag{1}$$

$$\bar{Y} = 2\omega j \frac{w_a l_a}{h_a}\left[\overline{\varepsilon_{33}^T} + \left(\frac{Za}{Z+Za}\right) d_{31}^2 \overline{Y_{11}^E}\left(\frac{\tan kl_a}{kl_a}\right) - d_{31}^2 \overline{Y_{11}^E}\right] \tag{2}$$

Harmonic analysis applied constant axial harmonic forces to the frame's PZT patch over a frequency range of 100 to 150 kHz. Displacements in the x-direction were measured at 1 kHz intervals. Equations 1 and 2 calculated structural impedance and electrical admittance. Initially, a 10 mm element size was used, then experiments were repeated with sizes of 5 mm, 4 mm, and 3 mm. Convergence in the conductance signature occurred with the 3 mm size, accurately representing the healthy condition. Figure 3 displays conductance profiles, demonstrating successful convergence with the 3 mm size.

3. Result and Discussion

Figure 5 exhibits Bhalla's signature [34]. This signature is used to compare study results. Through careful inspection and comparison of these indications, professionals may verify the numerical model's accuracy by comparing numerical conclusions to experimental data.

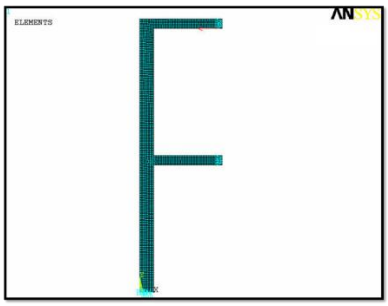

Fig 2. FE model of RC frame.

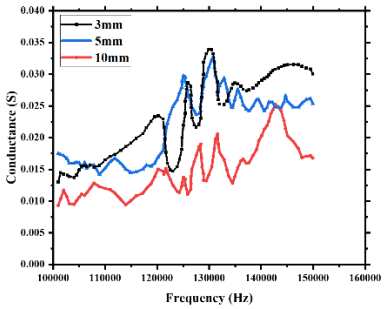

Fig 3. Conductance signatures with 3mm, 5mm, and 10mm elements.

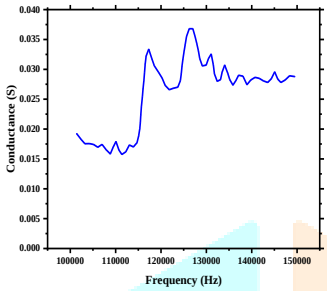

Fig 4. Numerical conductance signature of pristine frame model

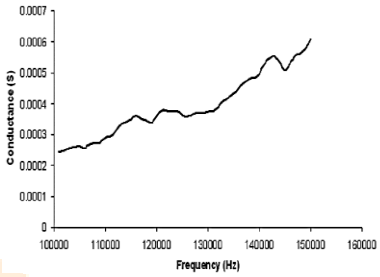

Fig 5. Experimental conductance signature of the pristine frame model [34].

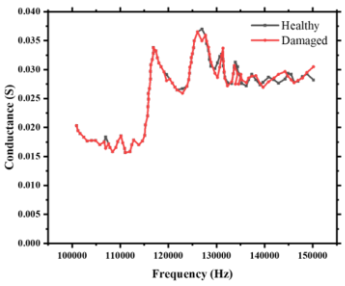

Fig.6 Conductance signature of healthy and damaged state from simulations.

Figures 4 and 5 show peak conductance values at frequencies that match computational expectations and experimental evidence. Given past discrepancies between experimental and simulated results, this congruence is notable. Our numerical model is supported by the 65-fold conductance magnitude disparity between calculated and experimental fingerprints. However, unexplained high-frequency effects and concrete damping property changes of 2% to 6% may cause inconsistencies. Research will improve the model's accuracy and prediction power to better comprehend structural dynamics and performance. Figure 6 compares the healthy structure's conductance signature to a slight vertical PZT flexural fracture. Unlike the healthy conductance signature, the damaged one travels vertically and laterally. Piezoceramic actuator/sensor patches monitor structural health by detecting structural deterioration. Engineering and research can detect and assess structural deterioration for early intervention and maintenance by measuring conductance signature changes. Diagnostic tools, signature alterations show structural integrity. This approach improves reliability and safety by monitoring and assessing the structure in real time using piezoceramic technology.

4. Damage impact on conductance signature of numerical model RC frame.

4.1 Impact of Flexural Crack

A purposeful flexural fracture was created at the frame's upper beam's most bending point. This was done by carefully lowering the components' Young's modulus at that time from 2.74E10 to 1E-06. Figure 7 shows the frame model with a flexural crack and its damage. To evaluate structural response to damage, PZT patch deformations were recorded within a preset frequency range. Figure 8 shows the damaged numerical frame's conductance signature. This signature shows how flexural fracture insertion affects structural behaviour, aiding structural health and integrity assessment. Figure 7 shows that the numerical model with flexural damage has conductance signature changes laterally to the right and vertically upward compared to the undamaged signature. Peak conductance also changes significantly. The damaged and undamaged models' conductance signatures had a 16.82% RMSD. This number quantifies the divergence between the two signatures caused by flexural damage. These findings show that the conductance signature may detect structural degradation, making it a useful structural health monitoring tool. The conductance signature alterations, peak conductance change, and RMSD value help explain the structural response to induced damage.

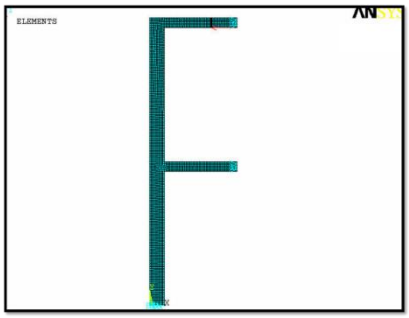

Fig 7. RC frame with flexural crack.

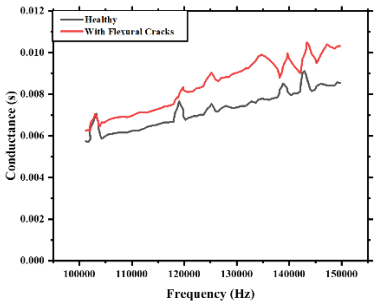

Fig 8. Conductance signatures due to flexural crack

4.2 Impact of Shear Crack

To execute the experiment, a 45˚ shear fracture was created near the upper beam's PZT patch. At that point, the components' Young's modulus was reduced. Figure 9 shows the shear-fractured RC frame. The shear fracture-simulated model conductance signature is displayed in Figure 10. Conductance signature represents structural response to shear fracture and frame dynamic behaviour. Researchers use this signal to study shear cracking's effects on frame health and structural integrity. Conductance signatures drop vertically with shear fractures (Figure 10). This signature change indicates shear damage. Conductance signature variations reflect structural state, showing the monitoring technique's shear damage sensitivity. Quantification gave this case a 15.74% RMSD index. This value confirms frame shear damage by measuring conductance signature discrepancy between damaged and uninjured structures. These findings prove conductance signatures may identify and measure structural degradation. The vertical downward shift and predicted RMSD index show shear damage's structural response, enabling maintenance and repair.

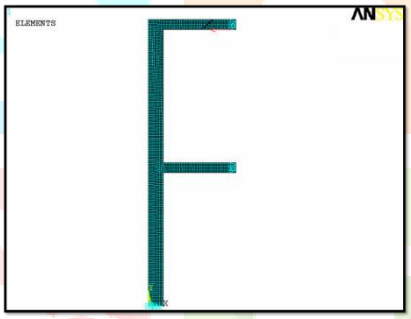

Fig 9. RC frame with shear crack.

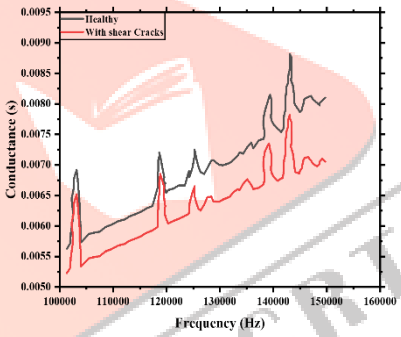

Fig 10. Conductance signatures due to shear crack

4.3 Impact of Flexural and Shear Cracks Together

Researchers carefully generated flexural and shear cracks at the same time and examined the conductance signature changes in the last step of the investigation. Figure 11 shows a frame with flexural and shear cracks to show the combined damage. Figure 12 shows the computational model's conductance signature, which includes flexural and shear cracks. Flexural and shear fractures cause a structural response that is represented by the conductance signature. This signature shows how these two forms of damage impact frame dynamics and integrity. Figure 12 shows that coupled flexural and shear fractures have a conductance profile within the range of signatures for their individual effects. This research shows that both types of damage affect the structural reaction, resulting in a composite signature. This sample has a 10.42% RMSD index. This value measures the conductivity signature difference between the frame with flexural and shear cracks and its undamaged state. The low RMSD index shows that flexural and shear fractures moderately change the conductance signature relative to the undamaged condition.

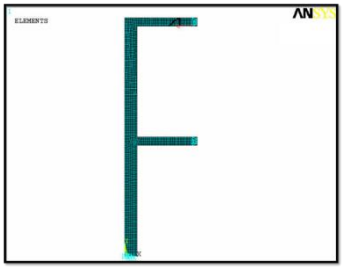

Fig 11. RC frame with both flexural and shear cracks.

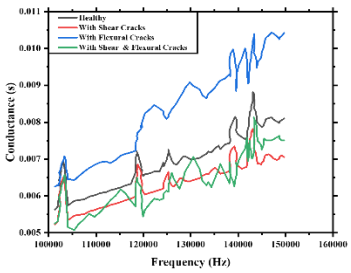

Fig 12. Conductance signatures due to flexural and shear crack together.

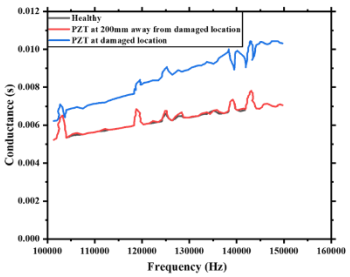

Fig 13. Impact of PZT distance from the damage location

4.4 Impact of PZT Distance from the Location of Damage

Figure 13 shows how the conductance signature varies with PZT-damage distance. This graphic reveals how the conductance signature is affected by the PZT patch's proximity to the damage location. By purposely varying the PZT-damage spot distance, researchers may test the monitoring approach's sensitivity to discover and assess structural damage at various spatial places inside the frame. Figure 13 shows that PZT patch degradation changes the conductance signature. The conductance signature modification rapidly decreases as the PZT patch and damage region distance rises. When positioned 200 mm from the injury, the PZT patch has no effect. This shows that damage detection requires the PZT patch to be close to the damage. Damage near the PZT patch allows the sensor to detect and characterise structural changes more sensitively. The sensor's capacity to detect damage decreases with distance between the PZT patch and the damage. These findings emphasise the importance of sensor location for structural health monitoring. Sensors near probable damage spots boost the monitoring system's sensitivity and capacity to identify and diagnose structural faults.

5. Comparison of Experimental and Simulated Results

Damage affects conductance signature experimentally, as seen in Figure 14. The frame experienced dynamic loading states 1–8 by changing frequency, velocity, and acceleration amplitude. Conductance patterns varied from baseline till stage 3. The signature increased steadily from condition 4 to state 6, suggesting damage. The conductance signature dropped significantly, and a break was seen at condition 7. At state 8, the fracture crossed the PZT patch, causing a sharp vertical conductance signature shift. These findings demonstrate the conductance signature's ability to identify structural degradation before visible damage. The conductance signature changes forecast damage early on, providing critical information about the frame's structural health and soundness. This shows that conductance-based structural health monitoring systems may detect degradation in real time.

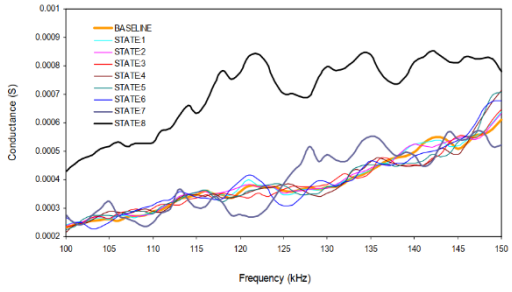

Fig 14. Experimental results [34].

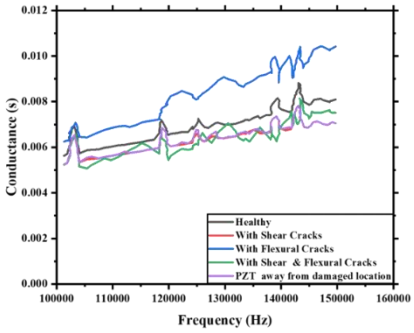

Fig 15. Results of Numerical model

The numerical results demonstrated that the conductance signature matched the experimental data shown in Figure 15. The baseline signatures differed from the experimental signatures by around 20, yet the patterns were constant. The conductance signature showed vertical upward and rightward lateral displacement due to flexural cracks at the maximum bending force. The conductivity signature dropped with shear cracks. When flexural and shear fractures coexisted, the conductance signature was intermediate between each crack type. Additionally, numerical study showed that the conductance signature can effectively identify damage within 150 mm of the PZT site. The PZT patch failed to identify damage at distances greater than this. The PZT

patch's closeness to the damaged region is crucial for conductance signature-based structural health monitoring systems to identify damage.

6. Conclusions

A lab-sized reinforced concrete frame Finite Element Model (FEM) was constructed using Bhalla and Soh's experimental data in ANSYS 9. Harmonic analysis was conducted at the PZT point with 100 kN of self-equilibrium harmonic forces from 100 to 150 kHz. The electrical admittance of PZT patches was calculated using translational displacements in the applied force direction at 1 kHz intervals, and the experimental conductance was compatible with the PZT patch signature. Peak conductance frequencies were identical in both signatures, indicating a strong dynamic relationship between the experimental frame and numerical model. Despite disparities in boundary effects, high-frequency analysis, and concrete attenuation uncertainty, the convergence of signature patterns demonstrated the numerical model's ability to replicate structural response and outperform data. Lowering element Young's modulus to induce construction cracks deteriorated state conductance signatures with time, showing damage consequences. The computational and experimental conductance profiles exhibited peak conductance at the same frequencies, suggesting cohesive structure and behavior. PZT patches detected damage 150 mm away, marking a significant advancement compared to previous studies. This numerical simulation proves more reliable than prior research, impacting intelligent infrastructure investigations by reducing experimental work, saving time and money, and facilitating structural health monitoring and damage identification. Numerical simulation extends the limits of PZT patch damage detection, allowing for expanded research without experimental constraints, ultimately advancing understanding of intelligent structures and structural health.

7. REFERENCES

[1]. Gudimetla A, Kumar P, Prasad SS, Geeri S, Sarath VV. Towards Smart Materials: Enhancing the Efficiency of the Materials. InModeling, Characterization, and Processing of Smart Materials 2023 (pp. 1-30). IGI Global.

[2]. Hassani FA, Shi Q, Wen F, He T, Haroun A, Yang Y, Feng Y, Lee C. Smart materials for smart healthcare–moving from sensors and actuators to self-sustained nanoenergy nanosystems. Smart Materials in Medicine. 2020 Jan 1;1:92-124.

[3]. Roy R, Bhakta D, Roy S. Applications and Types of Smart Materials. InModeling, Characterization, and Processing of Smart Materials 2023 (pp. 266-296). IGI Global.

[4]. Keshmiry A, Hassani S, Mousavi M, Dackermann U. Effects of environmental and operational conditions on structural health monitoring and non-destructive testing: A systematic review. Buildings. 2023 Mar 30;13(4):918.

[5]. Farrar, C. R., Sohn, H., Hemez, F. M., Anderson, M. C., Bement, M. T., Cornwell, P. J., Doebling, S. D., Lieven, N., Robertson, A. N., and Schultze, J. F. (2003) “Damage Prognosis: Current Status and Future Needs,” Los Alamos National Laboratory Report, LA-14051-MS.

[6]. Wang Y, Chen Y, Yao Y, Ou J. Advancements in Optimal Sensor Placement for Enhanced Structural Health Monitoring: Current Insights and Future Prospects. Buildings. 2023 Dec 17;13(12):3129.

[7]. Yao, J. T. P. (1985), “Saftey and Reliability of Existing Structures”, Pitman Publishing Programme, Boston.

[8]. Masciotta MG, Barontini A, Ramos LF, Amado-Mendes P, Lourenço PB. An overview on structural health monitoring: From the current state-of-the-art to new bio-inspired sensing paradigms. International Journal of Bio-Inspired Computation. 2019;14(1):1-26.

[9]. Bradshaw V. The building environment: Active and passive control systems. John Wiley & Sons; 2010 Sep 29.

[10]. Boscato G, Fragonara LZ, Cecchi A, Reccia E, Baraldi D. Structural health monitoring through vibration-based approaches. Shock and Vibration. 2019 Feb 17;2019.

[11]. Keshmiry A, Hassani S, Mousavi M, Dackermann U. Effects of environmental and operational conditions on structural health monitoring and non-destructive testing: A systematic review. Buildings. 2023 Mar 30;13(4):918.

[12]. Hassani S, Dackermann U. A systematic review of advanced sensor technologies for non-destructive testing and structural health monitoring. Sensors. 2023 Feb 15;23(4):2204.

[13]. Keshmiry A, Hassani S, Mousavi M, Dackermann U. Effects of environmental and operational conditions on structural health monitoring and non-destructive testing: A systematic review. Buildings. 2023 Mar 30;13(4):918.

[14]. Nainwal A. Innovative Use of Self-Healing Concrete for Sustainable Infrastructure. Mathematical Statistician and Engineering Applications. 2021 Jan 31;70(1):713-9.
[15]. Azimi M, Eslamlou AD, Pekcan G. Data-driven structural health monitoring and damage detection through deep learning: State-of-the-art review. Sensors. 2020 May 13;20(10):2778.
[16]. Cheng M, Fu Q, Tan B, Ma Y, Fang L, Lu C, Xu Z. Build a bridge from polymeric structure design to engineering application of self-healing coatings: A review. Progress in Organic Coatings. 2022 Jun 1;167:106790.
[17]. Lee MW, An S, Yoon SS, Yarin AL. Advances in self-healing materials based on vascular networks with mechanical self-repair characteristics. Advances in Colloid and Interface Science. 2018 Feb 1;252:21-37.
[18]. Ilyaei S, Sourki R, Akbari YH. Capsule-based healing systems in composite materials: A review. Critical Reviews in Solid State and Materials Sciences. 2021 Nov 2;46(6):491-531.
[19]. Yuan YC, Yin T, Rong MZ, Zhang MQ. Self healing in polymers and polymer composites. Concepts, realization and outlook: A review. Express polymer letters. 2008 Mar;2(4):238-50.
[20]. Wang W, Xiang Y, Yu J, Yang L. Development and prospect of smart materials and structures for aerospace sensing systems and applications. Sensors. 2023 Jan 31;23(3):1545.
[21]. Firoozi AA, Firoozi AA. Emerging Trends in Damage Tolerance Assessment: A Review of Smart Materials and Self-Repairable Structures. Structural Durability & Health Monitoring (SDHM). 2024 Jan 1;18(1).
[22]. Shakou LM, Wybo JL, Reniers G, Boustras G. Developing an innovative framework for enhancing the resilience of critical infrastructure to climate change. Safety science. 2019 Oct 1;118:364-78.
[23]. Beben D, Maleska T, Bobra P, Duda J, Anigacz W. Influence of traffic-induced vibrations on humans and residential building—a case study. International Journal of Environmental Research and Public Health. 2022 Apr 29;19(9):5441.
[24]. Singh MP, Elbadawy MZ, Bisht SS. Dynamic strain response measurement-based damage identification in structural frames. Structural Control and Health Monitoring. 2018 Jul;25(7):e2181.
[25]. Karbhari VM, Guan H, Sikorsky C. Operational modal analysis for vibration-based structural health monitoring of civil structures. InStructural health monitoring of civil infrastructure systems 2009 Jan 1 (pp. 213-259). Woodhead Publishing.
[26]. Haldar A, Das AK, Al-Hussein A. Data analysis challenges in structural health assessment using measured dynamic responses. Advances in Adaptive Data Analysis. 2013 Oct 6;5(04):1350017.
[27]. Pan H, Azimi M, Yan F, Lin Z. Time-frequency-based data-driven structural diagnosis and damage detection for cable-stayed bridges. Journal of Bridge Engineering. 2018 Jun 1;23(6):04018033.
[28]. Soleymani A, Jahangir H, Nehdi ML. Damage detection and monitoring in heritage masonry structures: Systematic review. Construction and Building Materials. 2023 Sep 15;397:132402.
[29]. Gharehbaghi VR, Noroozinejad Farsangi E, Noori M, Yang TY, Li S, Nguyen A, Málaga-Chuquitaype C, Gardoni P, Mirjalili S. A critical review on structural health monitoring: Definitions, methods, and perspectives. Archives of computational methods in engineering. 2022 Jun;29(4):2209-35.
[30]. Deng L, Cai CS. Applications of fiber optic sensors in civil engineering. Structural Engineering and Mechanics. 2007 Mar 30;25(5):577-96.
[31]. Ciang CC, Lee JR, Bang HJ. Structural health monitoring for a wind turbine system: a review of damage detection methods. Measurement science and technology. 2008 Oct 13;19(12):122001.
[32]. Glaessgen E, Stargel D. The digital twin paradigm for future NASA and US Air Force vehicles. In53rd AIAA/ASME/ASCE/AHS/ASC structures, structural dynamics, and materials conference 20th AIAA/ASME/AHS adaptive structures conference 14th AIAA 2012 Apr 23 (p. 1818).
[33]. Soleymani A, Jahangir H, Nehdi ML. Damage detection and monitoring in heritage masonry structures: Systematic review. Construction and Building Materials. 2023 Sep 15;397:132402.
[34]. Bhalla, S., Soh, C. K. (2004), “High frequency piezoelectric signatures for diagnosis of seismic/blast induced structural damages”, NDT&E International, Vol. 37, pp. 23–33.